



HAL
open science

Entanglement, Nonlinear Dynamics, and the Heisenberg Limit

Luca Pezzé, A. Smerzi

► **To cite this version:**

Luca Pezzé, A. Smerzi. Entanglement, Nonlinear Dynamics, and the Heisenberg Limit. *Physical Review Letters*, 2009, 102 (10), pp.100401. 10.1103/PhysRevLett.102.100401 . hal-00626569

HAL Id: hal-00626569

<https://hal-iogs.archives-ouvertes.fr/hal-00626569>

Submitted on 31 Mar 2016

HAL is a multi-disciplinary open access archive for the deposit and dissemination of scientific research documents, whether they are published or not. The documents may come from teaching and research institutions in France or abroad, or from public or private research centers.

L'archive ouverte pluridisciplinaire **HAL**, est destinée au dépôt et à la diffusion de documents scientifiques de niveau recherche, publiés ou non, émanant des établissements d'enseignement et de recherche français ou étrangers, des laboratoires publics ou privés.

Entanglement, Nonlinear Dynamics, and the Heisenberg Limit

Luca Pezzé* and Augusto Smerzi

BEC-CNR-INFM and Dipartimento di Fisica, Università di Trento, I-38050 Povo, Italy

(Received 29 November 2007; revised manuscript received 24 September 2008; published 10 March 2009)

We show that quantum Fisher information provides a sufficient condition to recognize multiparticle entanglement in an N qubit state. The same criterion gives a necessary and sufficient condition for sub-shot-noise phase sensitivity in the estimation of a collective rotation angle θ . The analysis therefore singles out the class of entangled states which are *useful* to overcome classical phase sensitivity in metrology and sensors. We finally study the creation of useful entangled states by the nonlinear dynamical evolution of two decoupled Bose-Einstein condensates or trapped ions.

DOI: 10.1103/PhysRevLett.102.100401

PACS numbers: 03.75.Gg, 03.65.Ud, 03.67.Bg, 03.75.Dg

Introduction.—The ability to create and manipulate entangled states of many-particle systems is a far-reaching possibility of quantum mechanics. Several efforts have been devoted, in the last few years, to exploiting entanglement to design new technologies for secure communication, metrology, and fast computation or to unveil foundational problems of quantum mechanics. From the experimental point of view, trapped Bose-Einstein condensates (BECs) [1,2], cold or thermal atoms [3], and trapped ions [4] are important candidates for the creation of large-scale quantum entanglement. It is important to emphasize, however, that not all entangled states are equally *useful* for developing protocols that outperform classical operations. Generally speaking, current measures of entanglement mostly focus on the algebraic separability properties of quantum states. This notion should be extended for quantum technological applications, where it is essential to classify entanglement on the basis of some additional physical or algebraic properties required by the specific task. These attributes are crucially related to nonseparability, but are not necessarily possessed by all entangled states.

In this Letter, we develop a general framework to study the interplay between entanglement and phase estimation in metrology and quantum sensors [5]. A quantum state $\hat{\rho}_{\text{inp}}$ must necessarily be entangled in order to be useful for estimating a phase shift θ with a sensitivity $\Delta\theta$ beyond the shot noise, which is the maximum limit attainable with separable states. Nevertheless not all entangled states can perform better than separable states. Here we introduce a new criterion, on a generic $\hat{\rho}_{\text{inp}}$, which is sufficient to recognize multiparticle entanglement and is necessary and sufficient for sub-shot-noise phase estimation sensitivity. We separate entangled states into two classes on the basis of an additional geometrical (or kinetic, see below) property in the Hilbert space. Our analysis uses basic tools of parameter estimation theory and provides a simple and experimentally measurable condition, Eq. (3), which extends other criteria discussed in the literature based on the concept of spin squeezing [1]. We will show, with an example experimentally achievable with dilute BECs and

trapped ions, how nonlinearity can generate a class of states which are entangled, useful for sub-shot-noise interferometry, but not spin squeezed.

A state of N particles in two modes (N qubits) is separable (nonentangled) when it can be written as [1,6]

$$\hat{\rho}_{\text{sep}} = \sum_k p_k \hat{\rho}_k^{(1)} \otimes \hat{\rho}_k^{(2)} \otimes \dots \otimes \hat{\rho}_k^{(N)}, \quad (1)$$

where $p_k > 0$, $\sum_k p_k = 1$, and $\hat{\rho}_k^{(i)}$ is the density matrix for the i th particle. How can entangled states be recognized? Let us introduce the “fictitious” angular momentum operator $\hat{J} = \sum_{l=1}^N \hat{\sigma}^{(l)}$, where $\hat{\sigma}^{(l)}$ is a Pauli matrix operating on the l th particle. According to the current literature, if a state $\hat{\rho}_{\text{inp}}$ satisfies the inequality

$$\xi^2 \equiv \frac{N(\Delta\hat{J}_{\vec{n}_3})^2}{\langle\hat{J}_{\vec{n}_1}\rangle^2 + \langle\hat{J}_{\vec{n}_2}\rangle^2} < 1, \quad (2)$$

then it is particle entangled [1,7,8] and spin squeezed [1,9,10] along the direction \vec{n}_3 , with \vec{n}_1 , \vec{n}_2 , and \vec{n}_3 three mutually orthogonal unit vectors and $\hat{J}_{\vec{n}_i} = \hat{J} \cdot \vec{n}_i$.

Here we introduce a different sufficient condition for particle entanglement:

$$\chi^2 \equiv \frac{N}{F_Q[\hat{\rho}_{\text{inp}}, \hat{J}_{\vec{n}}]} < 1, \quad (3)$$

where $F_Q[\hat{\rho}_{\text{inp}}, \hat{J}_{\vec{n}}] = 4(\Delta\hat{R})^2$ is the quantum Fisher information (QFI) [11–14] and \vec{n} is an arbitrary direction. The Hermitian operator \hat{R} is the solution of the equation $\{\hat{R}, \hat{\rho}_{\text{inp}}\} = i[\hat{J}_{\vec{n}}, \hat{\rho}_{\text{inp}}]$ [15]. It is possible to demonstrate that $\chi^2 \leq \xi^2$ [16]. Therefore, Eq. (3) recognizes a class of states which are entangled, $\chi^2 < 1$, and not spin squeezed, $\xi^2 \geq 1$, as, for instance, the maximally entangled state [8]. Notice that, for a pure state, $\hat{\rho}_{\text{inp}} = |\psi_{\text{inp}}\rangle\langle\psi_{\text{inp}}|$, we have $F_Q[\hat{\rho}_{\text{inp}}, \hat{J}_{\vec{n}}] = 4(\Delta\hat{J}_{\vec{n}})^2$ [11] and the sufficient condition for multiparticle entanglement, Eq. (3), assumes the appealing form

$$\chi_{\text{ps}}^2 \equiv \frac{N}{4(\Delta\hat{J}_{\vec{n}})^2} < 1. \quad (4)$$

The QFI is naturally related to the problem of phase estimation. Generally speaking, an interferometer is quantum mechanically described as a collective, linear, rotation of the input state by an angle θ : $\hat{\rho}_{\text{out}}(\theta) = e^{i\theta\hat{J}_{\vec{n}}}\hat{\rho}_{\text{inp}}e^{-i\theta\hat{J}_{\vec{n}}}$. The goal is to estimate θ with a sensitivity overcoming the shot-noise limit $\Delta\theta_{\text{sn}} \equiv 1/\sqrt{N}$. For instance, in Mach-Zehnder interferometry, θ is a relative phase shift among the two arms of the interferometer, and the rotation is about the $\vec{n} = \vec{y}$ axis.

For an arbitrary interferometer and phase estimation strategy, the phase sensitivity is limited by a fundamental bound, the Quantum Cramer-Rao (QCR) [12], which only depends on the specific choice of the input state,

$$\Delta\theta_{\text{QCR}} = \frac{1}{\sqrt{F_Q[\hat{\rho}_{\text{inp}}, \hat{J}_{\vec{n}}]}} = \frac{\chi}{\sqrt{N}}. \quad (5)$$

A comparison with Eq. (5) reveals that Eq. (3) is not only a sufficient condition for particle-entanglement, as already discussed, but also a necessary and sufficient condition for sub-shot-noise phase estimation. This is a main result of this work: $\chi < 1$ provides the class of entangled states which are *useful* for sub-shot-noise sensitivity. In other words, with chosen $\hat{\rho}_{\text{inp}}$ and $\hat{J} \cdot \vec{n}$, if the corresponding value of the QFI is such that $\chi < 1$, then the state is entangled, and if used as input of an interferometer realizing the unitary transformation $e^{-i\theta\hat{J}_{\vec{n}}}$, it provides a phase estimation sensitivity higher than any interferometer using classical (separable) states. On the other hand, the class of entangled states for which $\chi \geq 1$ cannot provide a sensitivity higher than the classical shot noise.

The QFI, which links Eqs. (3) and (5), has a simple interpretation as square of a “statistical speed,” $v_F^2 \equiv F_Q[\hat{\rho}_{\text{inp}}, \hat{J}_{\vec{n}}] = [dl(\theta)/d\theta]^2$. This corresponds to the rate of change of the absolute statistical distance $l(\theta)$ among two pure states in the Hilbert space (or in the space of density operators for general mixtures) along the path parametrized by θ [11,14]. The absolute statistical distance is the maximum number of distinguishable states along the path parametrized by θ , optimized over all possible generalized quantum measurements. According to Eq. (3), *useful* entanglement corresponds to high speed, $|v_F| > |v_{\text{cr}}|$, with $|v_{\text{cr}}| = \sqrt{N}$ a critical velocity that cannot be overcome by separable states. The maximum speed (strongest entanglement) is $|v_{\text{max}}| = N$, and therefore the fundamental (Heisenberg) limit in phase sensitivity is $\Delta\theta_{\text{HL}} = 1/N$. Physically, this simply means that, under the action of some unitary evolution, useful entangled states evolve (become distinguishable) more rapidly than any separable state.

Entanglement.—Let us introduce the inequalities

$$\frac{1}{M_{2k}(\theta)} \left(\frac{dM_k(\theta)}{d\theta} \right)^2 \leq F_Q[\hat{\rho}_{\text{inp}}, \hat{J}_{\vec{n}}] \leq 4(\Delta\hat{J}_{\vec{n}})^2, \quad (6)$$

where $M_k(\theta) \equiv \text{Tr}[\hat{M}^k \hat{\rho}_{\text{out}}]$, with \hat{M} an arbitrary observable [17]. The right-hand side of Eq. (6) allows us to demonstrate Eq. (3) by showing that $F_Q[\hat{\rho}_{\text{sep}}, \hat{J}_{\vec{n}}] \leq N$ for any arbitrary unit vector \vec{n} in the pseudo angular momentum space. First, notice that, for separable states, $\hat{\rho}_k = \hat{\rho}_k^{(1)} \otimes \hat{\rho}_k^{(2)} \otimes \dots \otimes \hat{\rho}_k^{(N)}$, we have $4(\Delta\hat{J}_{\vec{n}})^2 = N - 4\sum_{i=1}^N \langle \hat{J}_{\vec{n}}^{(i)} \rangle^2 \leq N$. Combining this result with Eq. (6) and the convexity of the QFI [16] (i.e., for an arbitrary mixture $\hat{\rho} = \sum_k p_k \hat{\rho}_k$, $F_Q[\hat{\rho}, \hat{J}_{\vec{n}}] \leq \sum_k p_k F_Q[\hat{\rho}_k, \hat{J}_{\vec{n}}]$), we obtain that $F_Q[\hat{\rho}_{\text{sep}}, \hat{J}_{\vec{n}}] \leq N$, where the equality sign can be saturated only with pure states. Moreover, since $4(\Delta\hat{J}_{\vec{n}})^2 \leq 4\langle \hat{J}_{\vec{n}}^2 \rangle \leq N^2$, we obtain $F_Q[\hat{\rho}_{\text{inp}}, \hat{J}_{\vec{n}}] \leq N^2$. Then, from Eq. (5), it follows that $\Delta\theta_{\text{HL}}$ is the highest possible phase sensitivity.

Using the left-hand side of Eq. (6) we now demonstrate that $\chi \leq \xi$ for any arbitrary $\hat{\rho}_{\text{inp}}$. We consider, without loss of generality, a direction $\vec{n} \equiv \vec{n}_2$ such that $\langle \hat{J}_{\vec{n}_2} \rangle = 0$. By choosing $\hat{M} = \hat{J}_{\vec{n}_3} - \langle \hat{J}_{\vec{n}_3} \rangle$ in Eq. (6), we obtain that $F_Q[\hat{\rho}_{\text{inp}}, \hat{J}_{\vec{n}}] \geq (dM_1/d\theta)^2/M_2 = N/\xi^2$. Then Eq. (3) shows that $\chi \leq \xi$: the class of states satisfying $\chi < 1$ is wider and includes the class of states defined by Eq. (2).

Nonlinear dynamics.—We now discuss the connection between nonlinear dynamics, entanglement, and spin squeezing. We consider a coherent spin state, $|j, j\rangle_{\vec{n}_1} = \sum_{\mu=-j}^{+j} \frac{1}{2^j} \sqrt{\binom{2j}{j-\mu}} |j, \mu\rangle_{\vec{n}_3}$ [18,19], with $j = N/2$. This state is separable ($\chi^2 = 1$), and we investigate the possibility of strongly entangling the particles by the nonlinear evolution $e^{-i\tau\hat{J}_{\vec{n}_3}^2}$. A direct calculation of Eqs. (2) and (3) with $\vec{n} \equiv \vec{n}_2$ (where the expectation values are computed over the state $|\psi(\tau)\rangle = e^{-i\tau\hat{J}_{\vec{n}_3}^2} |j, j\rangle_{\vec{n}_1}$) gives

$$\xi^2 = (\cos\tau)^{-2(N-1)}, \quad (7)$$

$$\chi^2 = 2/[(N+1) - (N-1)(\cos 2\tau)^{N-2}]. \quad (8)$$

Notice that $\xi^2 \geq 1$, while $\chi^2 \leq 1$ for all values of τ : the state $|\psi(\tau)\rangle$ is not spin squeezed but still (usefully) entangled. A comparison between Eq. (7) and Eq. (8) is presented in Fig. 1(a) for $N \gg 1$. We emphasize two time scales in the dynamical evolution of χ^2 : for $0 < \tau < 1/\sqrt{N}$, χ^2 decreases from 1 to $2/N$; for $1/\sqrt{N} \leq \tau \leq \pi/2 - 1/\sqrt{N}$, it reaches the plateau $\chi^2 = 2/N$. The dynamics are periodic with period $T = \pi/2$ for even values of N and $T = \pi$ for odd N (in which case $\chi^2 = 1/N$ at $\tau = \pi/2$).

Kitagawa and Ueda [10] have pointed out that the nonlinear evolution $e^{-i\tau\hat{J}_{\vec{n}_3}^2}$ actually creates spin squeezing, for $\tau \leq 1/\sqrt{N}$, along a particular direction. The maximum

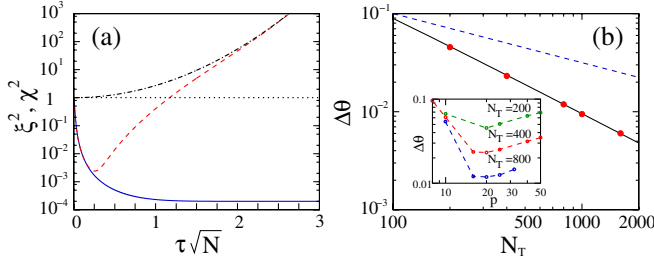


FIG. 1 (color online). (a) Plot of Eqs. (7) (dash-dotted black line), (8) (solid blue line), and (9) (dashed red line) as a function of $\tau\sqrt{N}$ (here $N = 10^4$). The states having χ^2 , $\xi^2 < 1$ (i.e., below the horizontal dotted line in the figure) are useful for quantum interferometry. (b) Phase sensitivity as a function of the total number of particles $N_T = Np$. Filled circles are results of numerical simulations, the solid black line is the Heisenberg limit $\Delta\theta = 8.9/N_T$, obtained for $p = p_{\text{opt}}$, and the dashed blue line is the shot noise $\Delta\theta = 1/\sqrt{N_T}$. Inset: $\Delta\theta$ as a function of the number of measurements p , for fixed values of N_T . The optimal working point (minimum of each curve) is $p_{\text{opt}} = 20$, independent from N_T .

squeezing is obtained for the state $|\tilde{\psi}(\tau)\rangle = e^{i\delta\hat{J}_{y1}}|\psi(\tau)\rangle$, where $\delta(N, \tau) = \frac{1}{2} \arctan \frac{B}{A}$, $A = 1 - (\cos 2\tau)^{N-2}$, and $B = 4 \sin \tau (\cos \tau)^{N-2}$. We have

$$\xi^2 = [4 + (N-1)(A - \sqrt{A^2 + B^2})]/4(\cos \tau)^{2N-2}. \quad (9)$$

Equation (9), as a function of τ , is shown in Fig. 1(a) [20]. We have $\xi^2 < 1$ for $0 < \tau \leq 1.15/\sqrt{N}$, and the minimum, $\xi_{\text{min}}^2 = 1/N^{2/3}$, is reached at $\tau = 1.2/N^{2/3}$. For $1/\sqrt{N} \leq \tau \leq \pi/2$, $\xi^2 > 1$ and it converges to Eq. (7), which eventually diverges at $\tau = \pi/2$.

Heisenberg limit.—So far we have demonstrated that the nonlinear evolution of a coherent spin state creates particle entanglement useful for sub-shot-noise sensitivity. This protocol has advantages when compared to the spin-squeezing approach discussed in [10] for improving the phase sensitivity of a Mach-Zehnder interferometer[21]. While spin squeezing is created only for short times, $\tau \leq 1/\sqrt{N}$, and along a direction $\delta(N, \tau)$ which strongly depends on τ and N , our scheme does not require any additional rotation of the initial state, is fairly independent on the evolution time, and reaches the Heisenberg limit [22], $\Delta\theta_{\text{HL}} = 1/N$, for times for $\tau \geq 1/\sqrt{N}$. Here we apply these results to a realistic BEC experimental setup. The coherent spin state can be created by splitting an initial condensate into two modes with the ramping of a potential barrier or by quickly transferring half of the particles from an initial condensate to two different hyperfine levels with a $\pi/2$ Bragg pulse. The nonlinear evolution, $e^{-i\tau\hat{J}_z^2}$, where $\tau = E_c t$, E_c is the charging energy, and t is the evolution time, is naturally provided by particle-particle interaction [23]. The nonlinear dynamics of an initial separable state has been also recently experimentally demonstrated with

trapped ions [4]. Here we consider a Mach-Zehnder interferometer with input state $|\psi(\tau)\rangle$ and infer the true value of the phase shift θ from the measurement of the relative number of particles at the output ports. These are characterized by conditional probabilities $P(\mu|j, \theta, \tau) = |\langle j, \mu | e^{-i\theta\hat{J}_y} |\psi(\tau)\rangle|^2$, with μ the result of a measurement. To achieve $\Delta\theta_{\text{QCR}}$, Eq. (5), we consider a Bayesian estimation scheme [24,25]. In Fig. 1(b) we plot the results of numerical simulations for $\tau = 1/\sqrt{N}$ and $\theta = \pi/2$. We show $\Delta\theta$ as a function of the total number of particles used in the estimation process $N_T = Np$, with $p = p_{\text{opt}} = 20$ the optimal number of independent measurements. The filled circles are numerical results [minima in the inset of 1(b)], and the solid line is $\Delta\theta = 8.9/N_T$. We notice that the more popular phase estimation scheme based on the measurement of average moments of \hat{J}_z [9] and the corresponding error propagation analysis only provide shot noise.

Can we understand the origin of sub-shot noise without spin squeezing? Let us investigate the phase structures characterizing the conditional probability distributions $P(\mu|j, \theta, \tau)$, defined for discrete values of $-j \leq \mu \leq j$. These distributions contain all of the available information

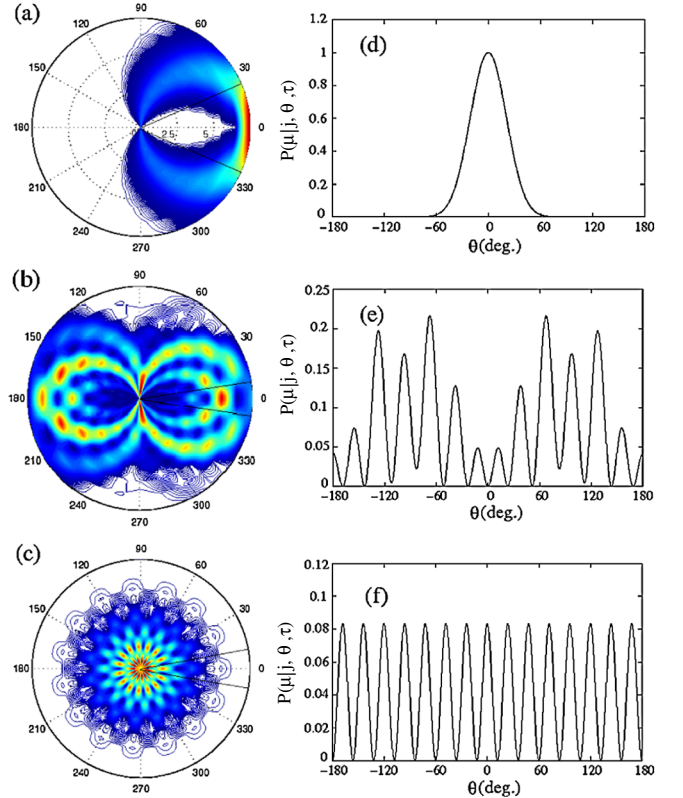


FIG. 2 (color online). (a–c) Distributions $P(\mu|j, \theta, \tau)$ plotted as a function of θ along circles of radius μ (taken as a continuum variable) at three different times during the nonlinear evolution: (a) $\tau = 0$, (b) $\tau = \pi/4$, and (c) $\tau = \pi/2$. The solid lines delimit the typical size of the substructures. (d–f) $P(\mu|j, \theta, \tau)$ as a function of θ , and for (d) $\tau = 0$, $\mu = 7.5$, (e) $\tau = \pi/4$, $\mu = 2.5$, and (f) $\tau = \pi/2$, $\mu = 3.5$. Here $N = 15$.

about the parameter θ that can be extracted from the measurement of μ . In Figs. 2(a)–2(c) we plot $P(\mu|j, \theta, \tau)$, as a function of θ , along circles of radius μ , at three different times during the nonlinear evolution: 2(a) $\tau = 0$, 2(b) $\tau = \pi/4$, and 2(c) $\tau = \pi/2$. The typical size of the substructures is $\sim 1/\sqrt{N}$ in 2(a) and $\sim 1/N$ in 2(b) and 2(c) as indicated, in the figure, by solid lines. This is also shown in Figs. 2(d)–2(f) where we plot $P(\mu|j, \theta, \tau)$ for different μ and the same τ as in Figs. 2(a)–2(c). The size of the relevant substructures indicates the smallest rotation angle needed to make the rotated state orthogonal to the initial one.

Conclusion.—We have explored the interplay between multiparticle entanglement and quantum interferometry. A key role is played by the quantum Fisher information. We obtained a sufficient condition for N -particles entanglement, $\chi < 1$ [Eq. (3)], which is more general than, and incorporates, the spin squeezing condition [Eq. (2)]. Large entanglement can be obtained through a nonlinear evolution and used to reach a phase sensitivity at the Heisenberg limit. Our results can have practical impact on precision spectroscopy, atomic clock, and atomic or optical interferometry, and can be implemented with Bose-Einstein condensates and trapped ions within the current technology.

*New address: Laboratoire Charles Fabry, Institut d'Optique, Campus Polytechnique, F-91127 Palaiseau cedex, France.

- [1] A. Sørensen *et al.*, Nature (London) **409**, 63 (2001).
- [2] J. Esteve *et al.*, Nature (London) **455**, 1216 (2008); K. Eckert *et al.*, Nature Phys. **4**, 50 (2008).
- [3] S. Chaudhury *et al.*, Phys. Rev. Lett. **99**, 163002 (2007); T. Fernholz *et al.*, *ibid.* **101**, 073601 (2008).
- [4] D. Liebfried *et al.*, Nature (London) **422**, 412 (2003); C. F. Roos *et al.*, *ibid.* **304**, 1478 (2004); K. Mølmer and A. Sørensen, Phys. Rev. Lett. **82**, 1835 (1999).
- [5] V. Giovannetti *et al.*, Science **306**, 1330 (2004).
- [6] A. Peres, Phys. Rev. Lett. **77**, 1413 (1996); R. F. Werner, Phys. Rev. A **40**, 4277 (1989).
- [7] G. Toth *et al.*, Phys. Rev. Lett. **99**, 250405 (2007); J. K. Korbicz *et al.*, *ibid.* **95**, 120502 (2005); X. Wang and B. C. Sanders, Phys. Rev. A **68**, 012101 (2003).
- [8] D. Ulam-Orgikh and M. Kitagawa, Phys. Rev. A **64**, 052106 (2001).
- [9] D. J. Wineland *et al.*, Phys. Rev. A **50**, 67 (1994).
- [10] M. Kitagawa and M. Ueda, Phys. Rev. A **47**, 5138 (1993).
- [11] S. L. Braunstein and C. M. Caves, Phys. Rev. Lett. **72**, 3439 (1994).
- [12] C. W. Helstrom, *Quantum Detection and Estimation Theory* (Academic Press, New York, 1976), Chap. VIII;
- A. S. Holevo, *Probabilistic and Statistical Aspect of Quantum Theory* (North-Holland, Amsterdam, 1982).
- [13] The Fisher information is defined as $F[\hat{\rho}_{\text{imp}}, \hat{J}_{\bar{n}}] \equiv \int d\eta \frac{1}{P(\eta|\theta)} \left(\frac{dP(\eta|\theta)}{d\theta}\right)^2$, where $P(\eta|\theta) \equiv \text{Tr}[\hat{E}(\eta)\hat{\rho}_{\text{out}}(\theta)]$, $\hat{E}(\eta)$ is a positive operator satisfying $\int d\eta \hat{E}(\eta) = \hat{1}$ (unit operator), and $\hat{\rho}_{\text{out}}(\theta) = e^{i\theta\hat{J}_{\bar{n}}} \hat{\rho}_{\text{imp}} e^{-i\theta\hat{J}_{\bar{n}}}$ is the rotated state. The QFI is $F_Q[\hat{\rho}_{\text{imp}}, \hat{J}_{\bar{n}}] \equiv \max_{\hat{E}(\eta)} F[\hat{\rho}_{\text{imp}}, \hat{J}_{\bar{n}}] = 2\sum_{j,k} \frac{(p_j - p_k)^2}{p_j + p_k} |\langle j|\hat{J}_{\bar{n}}|k\rangle|^2$, where $\{|j\rangle\}$ is an orthonormal set of states which diagonalizes $\hat{\rho}_{\text{imp}} = \sum_j p_j |j\rangle\langle j|$ (with $p_j \geq 0$ and $\sum_j p_j = 1$). The QFI can always be saturated by an optimal choice of $\hat{E}(\eta)$ [11].
- [14] W. K. Wootters, Phys. Rev. D **23**, 357 (1981).
- [15] For pure states, this equation is solved by $\hat{R} = i[\hat{J}_{\bar{n}}, \hat{\rho}_{\text{imp}}]$, and we have $(\Delta\hat{R})^2 = (\Delta\hat{J}_{\bar{n}})^2$. In general, $(\Delta\hat{R})^2 \leq (\Delta\hat{J}_{\bar{n}})^2$, and the equality is obtained only for pure states. S. Boixo and A. Monras, Phys. Rev. Lett. **100**, 100503 (2008); G. A. Durkin and J. P. Dowling, Phys. Rev. Lett. **99**, 070801 (2007); S. Luo, Phys. Rev. Lett. **91**, 180403 (2003).
- [16] L. Pezzé and A. Smerzi (to be published).
- [17] The upper bound of Eq. (6) has been derived in [11], while the lower bound can be demonstrated using the Cauchy-Schwarz inequality [16].
- [18] F. T. Arecchi *et al.*, Phys. Rev. A **6**, 2211 (1972).
- [19] $|j, \mu\rangle_{\bar{k}}$ are eigenstates of $\hat{J}_{\bar{k}}$ with eigenvalues $-j \leq \mu \leq j$.
- [20] Equation (3) calculated with $|\tilde{\psi}(\tau)\rangle$ gives $\chi^2 = 4/[4 + (N-1)(A + \sqrt{A^2 + B^2})]$ which, for $N \gg 1$, is similar to Eq. (8).
- [21] U. V. Poulsen and K. Mølmer, Phys. Rev. A **65**, 033613 (2002).
- [22] We refer to $\Delta\theta = \alpha/N$ as the Heisenberg limit of phase sensitivity, provided, of course, that the prefactor $\alpha \geq 1$ does not depend on N .
- [23] In two-mode approximation, the Hamiltonian of two independent BECs is $\hat{H} = E_c \hat{J}_z^2$, where E_c is the charging energy proportional to the particle-particle scattering length. It has been shown that the previous model provides a good approximation of the dynamics of the system. See A. S. Sørensen, Phys. Rev. A **65**, 043610 (2002).
- [24] L. Pezzé *et al.*, Phys. Rev. Lett. **99**, 223602 (2007).
- [25] We associate to the detection of a value μ the phase probability distribution $P(\phi|j, \mu) = P(\mu|j, \phi)P(\phi)/P(\mu)$ obtained from the Bayes theorem, where $P(\phi)$ is the prior knowledge (in the following $P(\phi) = 1/\pi$) and $P(\mu)$ provides the normalization. The Bayesian distribution associated to p independent measurements with results μ_1, \dots, μ_p is the product $P(\phi|j, \mu_1, \dots, \mu_p) \sim \prod_{i=1}^p P(\phi|j, \mu_i)$. The estimator θ_{est} is chosen as the maximum of $P(\phi|j, \mu_1, \dots, \mu_p)$, while phase sensitivity $\Delta\theta$ is the 68% confidence interval around θ_{est} .